A Machine Learning Approach to Automated Localization of Targets for Ventricular Tachycardia Ablation Using Sinus Rhythm Signal Features

Xuezhe Wang[1], Adam Dennis[1], Tarv Dhanjal[2], Pier D Lambiase[1,3], Michele Orini[1,4]

[1] Institute of Cardiovascular Science, University College London, United Kingdom
[2] University of Warwick, Honorary Consultant Cardiologist & Electrophysiologist, University Hospital Coventry & Warwickshire, United Kingdom
[3] Barts Heart Centre, Barts Health NHS Trust, London, United Kingdom
[4] School of Biomedical Engineering & Imaging Sciences, King's College London, United Kingdom

Abstract

Catheter ablation has the potential to become an effective treatment for ventricular tachycardia (VT), but the current identification of ablation sites relies on the operator's judgement and experience. This study proposes a novel machine learning approach to identify ablation targets based on signal features derived from intracardiac electrograms recorded in sinus rhythm. 56 substrate maps were collected during pacing and sinus rhythm using a multipolar catheter (Advisor HD grid, Ensite Precision) in 13 pigs with chronic myocardial infarction (n=31,515 mapping points). 36 VTs were induced and critical components of the VT circuit including early-, mid- and late-diastolic signals, were localized. Cardiac sites within 6 mm from these critical VT sites were considered as potential ablation targets (7.3% of all cardiac sites). 46 features representing signal morphology, function, spatial and spectral properties were extracted from each bipolar and unipolar signal recorded during pacing or sinus rhythm. A random forest algorithm was trained on 80% of the data to identify the 20 most important features and 10 times 10-fold cross-validation was used to identify the best model. Validation on the remaining 20% of data showed an area under the ROC curve of 77.8%, and both 70% of sensitivity and specificity, for the best model. This study demonstrates for the first time that machine learning may support clinicians in the localization of targets for VT ablation.

1. Introduction

Ventricular tachycardia is a life-threatening cardiac condition, and catheter ablation has the potential of becoming an effective and established treatment [1]. However, often more than half of the patients experience recurrence after the procedure due to the inability to accurately locate the critical points leading to VT during the electrophysiological study [2, 3]. A standard approach for the localization of ablation targets is to induce VT and to identify its critical components (early-, mid- and late-diastolic pathway) through pacing manoeuvres (e.g. entrainment) or activation mapping. Due to the limitation of being able to only map hemodynamically stable VTs, substrate mapping has been proposed as a safer and potentially more effective alternative. This consists of mapping ventricular electrical activity during sinus rhythm or pacing to identify arrhythmogenic properties closely related to potential components of VT circuits. Various signal metrics derived from substrate mapping have been shown to correlate with critical regions of VT circuit, such as, simultaneous amplitude frequency electrogram transformation [4], decrement evoked potential mapping [5], re-entry vulnerability index [6], but their accuracy remains limited. While machine learning and artificial intelligence are having a strong impact on the analysis of the body surface electrocardiogram (ECG) [7], little is known about their potential to improve targeted VT ablation. A recent study has shown that machine learning approaches can be used to accurately identify abnormal ventricular potentials [8], but their use for the identification of critical components of VT circuits remains unexplored. The potential relationship between signal features extracted from intracardiac electrograms (EGMs) and critical components of VT circuits also needs further research. The aim of this study was to develop a machine learning model based on substrate mapping features to predict the location of critical components of VT circuits.

2. Methods

2.1. Data collection and signal processing

Bipolar and unipolar signals used in this study were collected from 13 female Danish Landrace pigs, with a healed anterior myocardial infarct. An EnSite Precision 3D

cardiac mapping system (Abbott Medical, IL, USA) was used to collect 3D electroanatomical maps by programmed electrical stimulation (S1S2) and sensed extra (SE) pacing from the right (RV) and left (LV) ventricle, or both (BIV). The additional stimulus was delivered at least 20 ms above ventricular effective refractory period, following a sinus beat for SE and a series of drive trains with cycle lengths ranging between 400 and 600 ms for S1S2 stimuli. Sinus rhythm (SR) maps were created retrospectively from all clinical records segments. After substrate mapping, VT was indicted and VT activation mapping was performed for sustained haemodynamically tolerated tachycardias, with critical isthmus components (early-, mid- and late-diastolic signals) identified by dividing the diastolic period into 3 equal segments. We aimed to develop models able to identify the location of cardiac sites within 6 mm from 36 critical VT sites based on substrate mapping features. Figure 1 shows an example VT activation map with the corresponding SR substrate map from Pig 13.

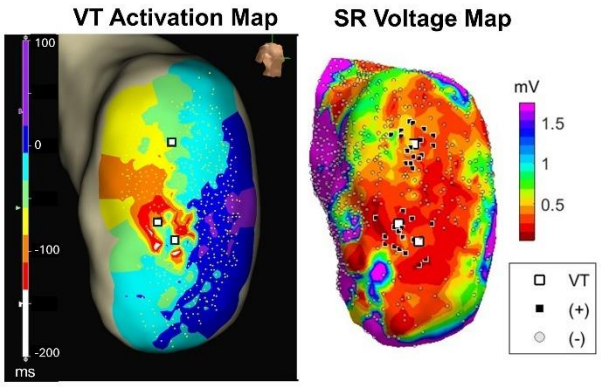

Figure 1. Left: Activation map during VT showing a re-entrant circuit with early-, mid- and late-diastolic signals (white squares). Right: Voltage map in SR indicating a large LV anterior scar. Black squares and grey circles represent sites which belong to the positive (within 6 mm from VT critical sites) and negative class, respectively.

The system collection window of the signals was 1000 ms. In order to accurately extract features from specific segments, all signals were trimmed after manual review to ensure that the starting point of the selected segment was just after the pacing artifact and before local ventricular activation. The duration of bipolar EGMs was set at 200 ms, while for unipolar EGMs this was set at 97.5 quartile of the repolarization time plus 30 ms. For both bipolar and unipolar EGMs, two windows of interest were defined as pre- and post-QRS, where the end of the QRS complex was identified from the 12-lead ECGs. The sampling frequency for EGMs was 2034.5 Hz and infinite Impulse Response band reject filter was used to eliminate 50±2 Hz electrical device noise. Unipolar and bipolar EGMs were band pass filtered between 0.50 – 500 Hz and 30 – 300 Hz, respectively. The location of EGMs to the 3D map was defined by the mapping system using actual coordinates in space.

2.2. Feature extraction

Features of the signals were extracted from bipolar and unipolar EGMs and categorized in four domains:

Functional domain: The following features were extracted from the signal morphology and relate to local electrophysiological properties: Activation time (AT) was measured by the mapping system as the latest deflection in the bipolar EGMs and was reviewed by an expert blinded to the study and corrected if required. Repolarization time (RT) was measured as the maximum of the first derivative of the unipolar electrogram's T-wave and activation-recovery interval (ARI), a surrogate for local action potential, was defined as $ARI = RT - AT$ [9]. Other features include the amplitude of the electrograms, and the mean and maximum of the absolute value of their first derivative ($\frac{d|U|}{dt}, \frac{d|B|}{dt}$), within and after the QRS complex. The duration of the EGMs and the number of deflections were also measured in both bipolar and unipolar signals.

Spatial domain: The spatial gradients of AT, RT and ARI ($GradAT, GradRT, GradARI$) were measured as the mean absolute change between neighbouring points within 10 mm divided by the distance between them. These features capture the spatial heterogeneity of conduction and repolarization, which are primary factors in arrhythmogenesis.

Spectral domain: Two features were included to capture signal properties that may not be assessed in the time-frequency domain: The first was the mean weighted frequency (f_{mean}), which was computed by the power spectral density estimated using Fast Fourier Transform. The second feature was the number of spectral peaks with minimum spacing as 5 Hz.

Time-frequency domain: Time-frequency properties of the bipolar signal have been shown to correlate with VT circuits [4]. The time-frequency spectrum of bipolar and unipolar EGMs was estimated using Cohen's class distributions [10] (with parameters $v_0 = 0.03, \tau_0 = 0.15, \lambda = 0.25$). Spectral power was calculated by averaging the time-frequency distribution in 8 time-frequency regions, constructed by dividing the temporal domain in QRS and post-QRS intervals. The frequency domain was then divided into spectral bands 40 Hz wide from 0 to 160 Hz for bipolar EGMs and 20 Hz wide from 0 to 80 Hz for unipolar EGMs. The power of each band was then normalized by the total energy of the signal.

Figure 2 shows the difference for some features between normal and critical VT sites.

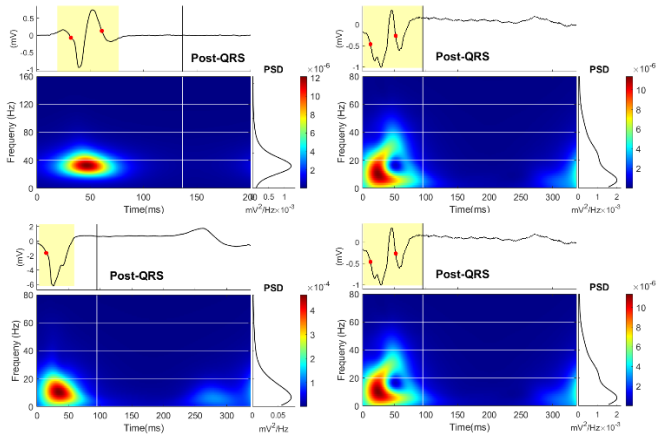

Figure 2. The top and bottom panels represent bipolar and unipolar EGMs, respectively, from the same substrate map. Left and right panels represent EGMs from normal sites and critical VT sites, respectively. The yellow region shows the signal duration (bipolar EGMs) and the duration of the QRS complex (unipolar EGMs), the red points represent signal deflections, and the black vertical line is the end of the QRS complex on the body surface ECG. The time-frequency distributions were divided in 8 regions.

2.3. Statistical Analysis

In total, 46 features were extracted. 30 features were log-transformed after manual check to reduce skewness and all continuous variables were normalized. Data from all maps were pooled together and 7 binary variables indicating the type of pacing strategy (Table 1) were included in the model. The positive class was composed of cardiac sites from substrate maps located within 6 mm from the 241 VT points, which from the 3 diastolic periods of the 36 VTs. To avoid data leakage, each VT point was treated as an individual during data partition with an 80%:20% ratio for training and test. The importance score for each feature was calculated based on Random Forest on training data and started by adding the feature with the highest score into the model [11]. Cross-validation (CV) was used to identify the best model. To address the impact of class imbalance, re-sampling strategies were proposed where the majority class was randomly under-sampled with a 1:1 and 1:5 positive: negative ratio. Default parameters were used in the Random Forest model in MATLAB, considering all features when splitting, with 100 trees ensembled, and the minimum number of samples in leaf equals to 1. The best performing model was assessed on the test set using accuracy, F1-score, positive predictive value (PPV), sensitivity, specificity, and area under the ROC curve (AUC), with the cut-off point closest to the upper left corner. 95% confidence intervals for AUC on the training set were calculated using bootstrapping, while CIs were not calculated on the test set since the sample number was too small.

3. Results

A total of 31,515 cardiac sites from substrate maps were included in the study, of which 2,305 points (7.3%) were marked as critical VT sites (Table 1). The model showed stable performance after adding the top 20 scoring features. The features with the highest score were RT, QRS duration and maximum changing rate during QRS complex from unipolar EGMs. The ARI, LAT, amplitude, and signals energy from both unipolar and bipolar EGMs were also included. No re-sampling strategy was performed as it can't improve the performance.

Table 1. Number of mapping points and VT critical sites for each pacing strategy. SR: Sinus Rhythm; RV: Right Ventricular; LV: Left Ventricular; BIV: Biventricular; SE: Sensed extra; S1S2: Programmed Simulation; N: Number of Maps; Q2(Q1-Q3): Median (1^{st} quartiles-3^{rd} quartiles).

Map	N	Signal Points Per Map	VT critical sites
SR	10	1091(543-1649)	69(51-86)
RV (SE)	10	625(452-727)	40(15-51)
RV (S1S2)	10	284(157-431)	26(9-39)
LV (SE)	10	577(402-867)	46(16-88)
LV (S1S2)	5	320(226-366)	16(1-29)
BIV (SE)	8	281(194-469)	34(18-49)
BIV(S1S2)	3	184(177-283)	16(5-59)
Total	**56**	**460(257-741)**	**32(15-61)**

The average performance of the model assessed in 10 times 10-fold CV is shown in Table 2. On the under-sampled training set, the AUC was 72.9% [95%CI: 71.9%-73.9%]. Accuracy, specificity, and sensitivity were all close to 70%, while the F1-score and PPV were lower, at 23.8% and 14.5%, respectively.

In the test set with the best model selected during training showed an AUC equal to 77.8%; accuracy, specificity, and sensitivity were all equal or over 70%. F1-score and PPV were 24.9% and 15.1%.

Table 2. Average performance during 10 times 10-fold CV for Random Forest on training and the best model on test set.

	Training (±SD)	Test
AUC	72.9% [CI: 71.9%-73.9%]	77.8%
Accuracy	67.0±4.4%	70.0%
F1-score	23.8±3.9%	24.9%
PPV	14.5±2.8%	15.1%
Specificity	67.9±5.6%	70.2%
Sensitivity	68.0±4.7%	70.0%

4. Discussion and Conclusion

The aim of this study was to develop a machine learning approach to accurately identify critical components of the VT circuit based purely on substrate map EGMs to guide ablation. As an advanced ensemble algorithm, Random Forest model was trained on multi-domain features from bipolar and unipolar EGMs recorded using a state-of-the-art 3D mapping system in sinus rhythm or pacing. Using 20 selected features capturing functional, spatial, spectral, and time-frequency properties, the model was able to predict the location of VT critical sites with an AUC close to 80%. The model showed stability and high performance even on the extremely unbalanced test set, which reflected a real case scenario. To the best of our knowledge, this study is the first study to propose a machine learning approach for the identification of VT ablation targets, which could support clinicians in eliminating critical substrate without having to induce VT. This strategy also has the potential to identify novel markers of increased vulnerability to re-entry by revealing associations between novel signal features and critical VT sites.

A relatively low F1-score and PPV indicate that the model may predict a substantial number of false positive sites. This is however expected in cases where there is a large imbalance between normal cardiac sites and cardiac sites which may be critical components of a potential unmapped VT circuit. Indeed, for fixed sensitivity and specificity levels, the PPV dramatically decreases for decreasing prevalence [12]. The under-sample strategies provided a similar result to the original ratio, but other solutions may be developed to improve the performance in the future. In this study, we have pooled together features from different substrate maps conducted in the 13 pigs, which may have resulted in some degree of pseudo-replication. We included the type of substrate map as a predictor to alleviate this problem, but other solutions may be tested in further research. We used the default random forest parameters, and optimization of hyperparameters may further improve the model performance. Furthermore, our machine learning approach could be adopted to compare different substrate mapping strategies (e.g. sinus rhythm and different pacing configurations). Finally, extrapolating our methodology to deep learning methods, such as convolutional neural network [13] which is directly applied to intracardiac EGMs without requiring feature extraction, may further enhance identification of VT ablation targets.

References

[1] Á. Arenal *et al.*, "Substrate Ablation vs Antiarrhythmic Drug Therapy for Symptomatic Ventricular Tachycardia," *Journal of the American College of Cardiology*, vol. 79, no. 15, pp. 1441–1453, Apr. 2022.

[2] B. K. Martinez *et al.*, "Systematic Review and Meta-analysis of Catheter Ablation of Ventricular Tachycardia in Ischemic Heart Disease," *Heart Rhythm*, vol. 17, no. 1, pp. e206–e219, Jan. 2020.

[3] A. Breitenstein *et al.*, "Ventricular Tachycardia Ablation in Structural Heart Disease: Impact of Ablation Strategy and Non-inducibility as an End-point on Long Term Outcome," *International Journal of Cardiology*, vol. 277, pp. 110–117, Feb. 2019.

[4] C.-Y. Lin *et al.*, "Simultaneous Amplitude Frequency Electrogram Transformation (SAFE-T) Mapping to Identify Ventricular Tachycardia Arrhythmogenic Potentials in Sinus Rhythm," *JACC: Clinical Electrophysiology*, vol. 2, no. 4, pp. 459–470, Aug. 2016.

[5] Andreu Porta-Sánchez *et al.*, "Multicenter Study of Ischemic Ventricular Tachycardia Ablation With Decrement-Evoked Potential (DEEP) Mapping With Extra Stimulus," *JACC: Clinical Electrophysiology*, vol. 4, no. 3, pp. 307–315, Mar. 2018.

[6] M. Orini et al., "Evaluation of the Reentry Vulnerability Index to Predict Ventricular Tachycardia Circuits Using High-density Contact Mapping," *Heart Rhythm*, vol. 17, no. 4, pp. 576–583, Apr. 2020.

[7] K. C. Siontis, P. A. Noseworthy, Z. I. Attia, and P. A. Friedman, "Artificial Intelligence-enhanced Electrocardiography in Cardiovascular Disease Management," *Nature Reviews Cardiology*, vol. 18, no. 7, pp. 465–478, Feb. 2021.

[8] G. Baldazzi, M. Orrù, G. Viola, and D. Pani, "Computer-aided Detection of Arrhythmogenic Sites in Post-ischemic Ventricular Tachycardia," *Scientific Reports*, vol. 13, no. 1, p. 6906, Apr. 2023.

[9] M. Orini, N. Srinivasan, A. Graham, P. Taggart, and P. D. Lambiase, "Further Evidence on How to Measure Local Repolarization Time Using Intracardiac Unipolar Electrograms in the Intact Human Heart," *Circulation: Arrhythmia and Electrophysiology*, vol. 12, no. 11, Nov. 2019.

[10] M. Orini, R. Bailon, L. T. Mainardi, P. Laguna, and P. Flandrin, "Characterization of Dynamic Interactions Between Cardiovascular Signals by Time-Frequency Coherence," *IEEE Transactions on Biomedical Engineering*, vol. 59, no. 3, pp. 663–673, Mar. 2012.

[11] R.-C. Chen, C. Dewi, S.-W. Huang, and R. E. Caraka, "Selecting Critical Features for Data Classification Based on Machine Learning Methods," *Journal of Big Data*, vol. 7, no. 1, Jul. 2020.

[12] D. G. Altman and J. M. Bland, "Diagnostic Tests 2: Predictive Values," *BMJ*, vol. 309, pp. 102, July 9, 1994.

[13] A. Mjahad, M. Saban, H. Azarmdel, and A. Rosado-Muñoz, "Efficient Extraction of Deep Image Features Using a Convolutional Neural Network (CNN) for Detecting Ventricular Fibrillation and Tachycardia," *Journal of Imaging*, vol. 9, no. 9, p. 190, Sep. 2023.

Address for correspondence:
Xuezhe Wang
1-19 Torrington Place, London, United Kingdom
rmhixwa@ucl.ac.uk